Monatomic Au wire with a magnetic Ni impurity: Electronic structure and ballistic conductance

Yoshio Miura,[1] Riccardo Mazzarello,[2,3,*] Andrea Dal Corso,[2,3] Alexander Smogunov,[3,4,5] and Erio Tosatti[2,3,4]
[1]*RIEC, Tohoku University, Katahira 2-1-1, Aoba, Sendai 980-8577, Japan*
[2]*SISSA, Via Beirut 2/4, Trieste 34014, Italy*
[3]*INFM, Democritos, Unitá di Trieste, Via Beirut 2/4, Trieste 34014, Italy*
[4]*ICTP, Strada Costiera 11, Trieste 34014, Italy*
[5]*Voronezh State University, University Square 1, Voronezh 394006, Russia*
(Received 2 September 2008; revised manuscript received 15 October 2008; published 10 November 2008)

The influence of a magnetic impurity (Ni atom) on the electronic, magnetic, and Landauer conductance properties of a monatomic Au wire is studied by first-principles density-functional calculations. We compare two adsorption geometries: bridge and substitutional. We find that the Ni atom remains magnetic in both cases; however, in the bridge geometry, the total spin is close to 1/2 and the symmetry of the hole is $d_{3z^2-r^2}$ while in substitutional it is larger than 1/2 with two degenerate holes with symmetry d_{yz} and d_{zx}. By using the Büttiker-Landauer theory, we find that in the first case the ideal, frozen spin conductance is somewhat diminished by the Ni impurity, although quite sensitive to calculation details such as the position of the empty Ni *d* and *s* states, while in the substitutional case conductance remains close to the ideal value G_0 $(=2e^2/h)$ of the pristine gold wire.

DOI: 10.1103/PhysRevB.78.205412 PACS number(s): 73.63.Rt, 73.23.Ad, 73.40.Cg

I. INTRODUCTION

A good understanding and control of electronic and transport properties of atomic-size conductors is a must in modern nanoscience, where one goal is to build structures with novel functionalities exploiting the possibilities offered by the nanosize of these components. Atomic-size contacts and nanowires are routinely produced by scanning tunneling microscopes and by mechanically controllable break junctions.[1] Since the electron mean-free path is larger than the size of these structures, their conductance is ballistic and quantized with values that are material dependent. For instance, in noble metals (Cu, Ag, and Au) the ultimate conductance plateau corresponding to a monatomic contact or a monatomic nanowire has a value close to G_0 $(G_0=2e^2/h)$,[2–5] corresponding to essentially perfect transmission of two wide-band *s* electrons (one for each spin) across the contact. In transition metals instead (Fe, Ni, Co),[2,6–9] the lowest conductance plateau is generally larger than G_0 and more difficult to explain. Here, in fact, in addition to the *s* channel there is a conductance contribution from the 3*d* electrons. Their narrower bandwidth, however, yields a conductance contribution per channel well below G_0. Moreover these metals are ferromagnetic, and magnetism plays a role in determining the conductance, which becomes strongly spin polarized, generally higher for minority spins.[10]

An interesting geometry to consider is a noble-metal nanocontact with a transition-metal impurity. Due to the reduced coordination, the impurity will generally develop a magnetic moment. We will assume in the present work that this moment is frozen and nonfluctuating, such as one would obtain with a strong external magnetic field. The *s* electrons from the noble-metal contacts will impinge on the impurity, suffering partial reflection as well as transmission, both of course spin polarized. How will the spin-polarized *d* electrons of the impurity influence the conductance of the nanocontact? In addition, how will this effect depend on the impurity geometry? We choose to address these questions in the simplest idealized system, consisting of a monatomic noble-metal nanowire with a single transition-metal impurity.

Recently, the conductance of noble-metal nanowires with transition-metals impurities [Au nanowires with Pd (Ref. 11) and Cu nanowires with Ni (Ref. 12)] has been studied experimentally using point-contact techniques. Pd addition to Au nanowires leads merely to a height decrease in the G_0 peak in the conductance histogram but no shift has been observed, at least in Au-rich nanowires. Low concentrations of Ni on a Cu nanowire (generally nonmonatomic, however) act as impurity scatterers for the electrons and lead to a decrease in the conductance resulting in a small shift toward lower values of the peaks in the conductance histogram.

Theoretical studies of the ballistic conductance in these systems are still rare.[13–15] Calculations performed on metallic Cu nanowires with the diameter of a few atoms in presence of transition-metal impurities suggested a spin-dependent conductance with several transition metals, but found that Ni impurities become nonmagnetic. By simulating the conductance of Au(001) point contacts, with transition-metal impurities (Pd, Fe, and Co) placed on various positions near the center of the point contact,[14] it was found that the conductance is very sensitive to the position of the magnetic impurity. The changes in conductance were mainly attributed to the minority *d* bands of the impurity which modify the *s*-like density of states at the center of the point contact. In Ref. 15 it was shown that the transport properties of Au nanowires with a Co atom constriction are spin dependent and are strongly affected by the local symmetry of the system.

The main goal of this paper is to understand the spin-dependent scattering in a noble-metal monoatomic wire with a transition-metal impurity. We consider a long chain of Au atoms[16,17] with a Ni impurity in it and we study two geometries: Ni adsorbed on the bridge position or as a substitutional impurity. We discuss the bonding mechanism of the Ni impurity to the gold wire as well as its magnetic properties and its effects on the ballistic conductance. Our calculations

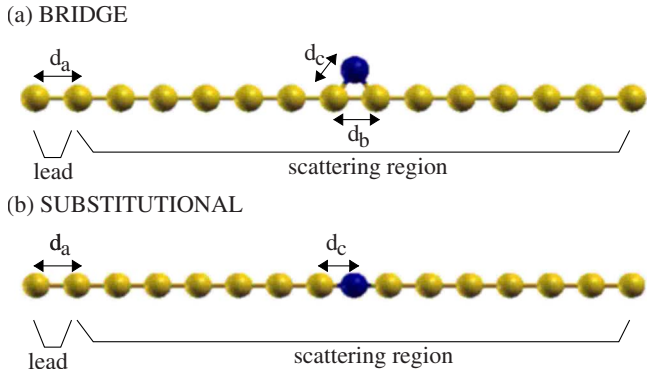

FIG. 1. (Color online) Supercells of monoatomic linear Au_{15} wires with a Ni impurity (a) for the bridge case and (b) the substitutional case.

are carried out within a density-functional theory (DFT) approach combined with the Landauer-Büttiker formalism,[18] using the method originally proposed by Choi and Ihm[19] for the Kleinman-Bylander-type pseudopotentials and generalized[10,20] to the ultrasoft pseudopotential scheme.[21] Generalized-gradient approximation (GGA)+U calculations[22] were also carried out to verify qualitatively the effect of strong correlations on the positions of the energy levels and their consequent influence on conductance.

We find that as expected the Ni impurity develops a magnetic moment in both geometries. In the bridge configuration, it modifies the transmission of gold s electrons near the Fermi level in a spin-dependent way. The precise value of the ballistic conductance is difficult to predict since it is quite sensitive to the details of the calculation, such as the exact position of the empty Ni d and s states, which in turn is imprecise in DFT, as shown by the GGA+U calculation. In the substitutional case, where the magnetic moment is even larger, the transmission of gold s electrons is surprisingly spin independent due to symmetry. Here the predicted conductance is therefore only slightly reduced with respect to the clean gold wire. The transmission of the filled gold d channels is also found to be sensitive to the details of the interaction and spin dependent. However, these states lie below the Fermi level and do not contribute to the equilibrium ballistic conductance.

II. METHODS

Our calculations are done within DFT using the spin-polarized generalized-gradient approximation (σ-GGA) with the Perdew-Burke-Ernzerhof parametrization[23] of the exchange and correlation energy. The nuclei and core electrons are described by ultrasoft pseudopotentials[21] and the wave functions are expanded in a plane waves basis set. We use kinetic-energy cutoffs of 30 and 300 Ry for the wave functions and the charge density, respectively. All calculations are done by the QUANTUM ESPRESSO code.[24] We consider a supercell containing a linear monatomic Au wire with 16 atoms and one Ni atom (see Fig. 1). The supercell is repeated periodically in the xy plane with a wire-wire distance of 10.58 Å, a distance checked to be large enough to avoid artificial interactions between the periodic replicas of the wire. The integration of the one-dimensional (1D) Brillouin zone is done on a uniform mesh of ten k points while the presence of a Fermi level is dealt with by the Methfessel-Paxton broadening technique[25] with a smearing parameter of 0.002 Ry. The projected density of states are calculated in a supercell containing 40 Au atoms in order to hide small artificial gaps due to the periodic replicas of the Ni atom.

Ballistic conductance is given in the Landauer-Büttiker approximation by $G=(e^2/h)T(E_F)$, where $T(E_F)$, the total transmission at the Fermi energy, can be expressed as $T(E_F)=\mathrm{Tr}[\mathbf{t}^\dagger\mathbf{t}]$, where $\mathbf{t}$ is the matrix of normalized transmission amplitudes. Transmission as a function of energy is calculated by the method by Choi and Ihm[19] generalized to ultrasoft pseudopotential[10] by solving the scattering equation in an open quantum system composed by two semi-infinite leads and a scattering region. The lead and scattering regions of our system are shown in Fig. 1.

The self-consistent potential in the first part of the supercell of length equal to the Au-Au distance is used to build the periodic potential of the left and right leads, while the potential in the rest of the supercell is used for the scattering region. Therefore the leads start at a distance of about 22 Å away from the Ni atom. At this distance the perturbation caused by the Ni atom is very small, and the electron bands at real wave vector k calculated using this potential agree with the bands of the perfect wire within 0.01 eV. The ballistic conductance is estimated by the Landauer formula[18] (zero-bias limit), calculating the transmission at the Fermi level. All spin moments are assumed to be frozen, excluding all fluctuations and possible Kondo effects, as if under a strong magnetic field.

III. RESULTS

A. Structural properties

In Fig. 1, we show the two geometries considered in this work. Figure 1(a) shows the bridge geometry while Fig. 1(b) shows the substitutional geometry where one Au atom is replaced by a Ni atom. In the bridge case, we assume that the Ni impurity lies in the xz plane. The structural parameters d_b and d_c for the bridge case and d_c for the substitutional case are obtained by optimizing the atomic positions of the Ni atom and of the two Au atoms closer to the Ni and changing the longitudinal size of the supercell until the minimum energy is found. During the optimization, the Au-Au bond length (d_a) for all the other atoms is fixed to the value d_a =2.80 Å. A value of d_a larger than the equilibrium distance was chosen because at shorter d_a (in particular, at the equilibrium Au-Au bond length, 2.60 Å), DFT calculations yield a slightly magnetic Au wire:[26] this spurious magnetization is due to self-interaction errors, which shift the $m=1$ band of the Au wire up to the Fermi energy.[27]

The calculated values of d_b and d_c are reported in Table I. On the same table we also report the total magnetization of the system and an estimate of the adsorption energies E_{ad}, calculated as the difference between the energy of the Au wire with a Ni impurity and the sum of the energies of the clean Au wire and of the isolated Ni atom [assumed in the

TABLE I. The table shows the adsorption energy (E_{ad}), total magnetization (M_{tot}), and Au-Au (d_b) and Au-Ni (d_c) bond lengths for the bridge case and the substitutional case. Corresponding E_{ad} and d_c for Ni adsorbed on the hcp-hollow site of Au(111) are also shown for comparison.

Position	Bridge	Subst.	Au(111)
E_{ad} [eV]	3.47	2.56	3.33
M_{tot} [μ_B]	1.30	1.93	
d_b [Å]	2.74		
d_c [Å]	2.42	2.37	2.49

$3d^9 4s^1$ configuration, which is the ground state in the local density approximation (LDA)], with fully occupied $3d$ spin-up states and four electrons in the $3d$ spin-down states. We also calculated E_{ad} and d_c for Ni adsorbed on the hexagonal close packed (hcp)-hollow site of Au(111); these quantities are reported in Table I as well. It is found that the Ni atom prefers to adsorb on the bridge site rather than on the substitutional site of the monoatomic Au wire, most likely because the latter involves the breaking of a Au-Au bond. The adsorption energy $E_{ad}=3.47$ eV on the bridge site is slightly larger than the value 3.33 eV found for Ni adsorbed on the hcp-hollow site of the Au(111) surface. The substitutional site has an adsorption energy of 2.56 eV. While energetically less stable than the bridge site, the substitutional geometry is worth considering both because of its different symmetry and because it could be realized under large stress. Experimentally the Au nanowire can in fact sustain a large finite tension of 1.5 nN,[28,29] and the substitutional configuration could become energetically favorable just before breaking.

B. Magnetic properties

In Fig. 2, we show the planar average of the magnetization density integrated on xy planes as a function of z along the wire. The local magnetic moment of Ni is estimated by integrating the planar average from $(z_{Ni}+z_{Au,l})/2$ to $(z_{Ni}+z_{Au,r})/2$, where z_{Ni} is the z coordinate of Ni and $z_{Au,l}$ ($z_{Au,r}$) are the z coordinates of the Ni nearest-neighbor left (right) Au atoms. The values found in this way, $1.06\mu_B$ and $1.36\mu_B$, respectively, for bridge and substitutional geometries, are larger than the calculated moment of bulk fcc-Ni ($0.61\mu_B$) but significantly smaller than that of the isolated atom ($2\mu_B$). This indicates that when the Ni atom is adsorbed on the wire, there is a substantial difference in the charge transfer in the two spin channels (see below). The larger value with respect to the bulk can be attributed to the low coordination of the Ni atom. In particular, the local magnetic moment of Ni for the bridge case is smaller than for the substitutional case, and is similar to that calculated for an infinite monatomic Ni wire ($1.11\mu_B$).[30] Furthermore, the two Au atoms nearest neighbor to Ni develop a small induced magnetic moment of $0.10\mu_B$ and $0.19\mu_B$ for the bridge and substitutional case, respectively, with the same sign as that of Ni.

In Fig. 3, we show the spin-resolved charge-density transfer $\Delta\rho(r)=\rho_{Ni/Au-wire}(r)-[\rho_{Ni}(r)+\rho_{Au-wire}(r)]$ for both bridge and substitutional cases. In this simulation the atomic configuration of the isolated Ni atom is taken to be $3d^8 4s^2$, which is the experimental ground state of the isolated atom. Charge flows from the black (negative) region to the white (positive) region. In Fig. 3(a), which corresponds to the bridge structure, we can see a charge transfer from the Ni atom to the Au wire in the majority-spin part. In particular, the majority-spin $\Delta\rho(r)$ around the Ni atom shows an s-like negative spatial distribution, indicating that the Ni atom loses s-electron charge that goes to the Au wire. On the other hand, in the minority-spin $\Delta\rho(r)$ the charge flows from the Au wire to Ni-Au bonding region because partially occupied Ni d states acquire additional electrons making bonds with the fully occupied Au d states. A similar charge transfer can be observed in the $\Delta\rho(r)$ for the substitutional case in Fig. 3(b), and strong hybridization between Ni d and Au d states is evident as compared with the bridge case.

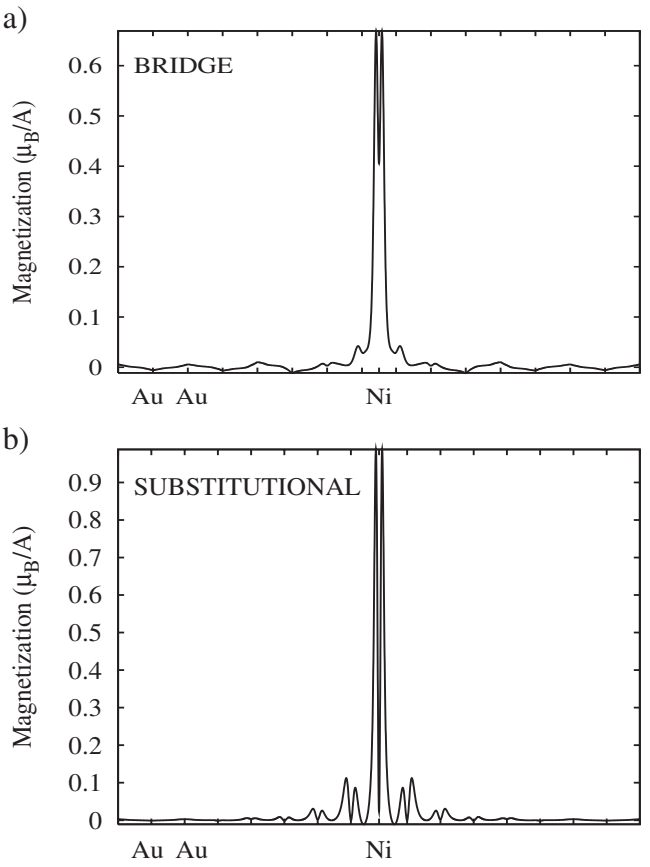

FIG. 2. Planar average of the magnetization density integrated on the xy plane and plotted along z for (a) the bridge and (b) the substitutional case. The tics on the $\hat{x}$ axis indicate the positions of the atoms.

C. Electronic structure

We show in Figs. 4–6 the projected density of states (PDOS) on the Ni orbitals and the PDOS on the atomic orbitals of the two Au atoms close to the Ni. In the latter, the PDOS of the clean monatomic Au wire are also shown for comparison. Figure 4 (Fig. 5) corresponds to states of the

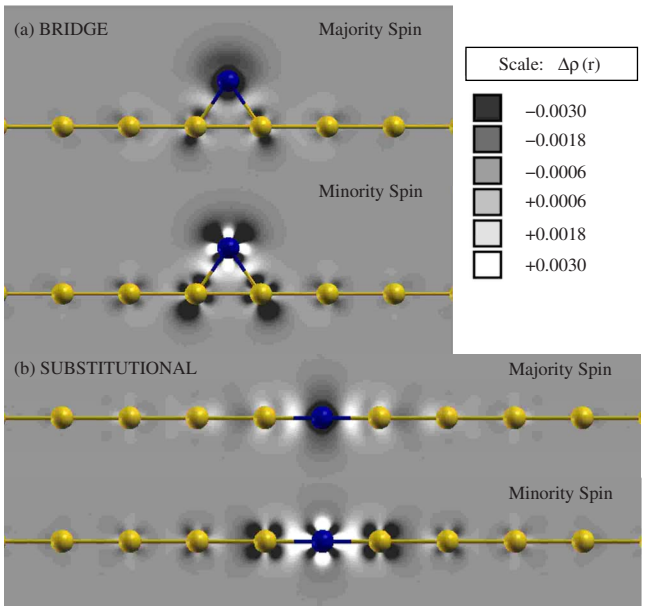

FIG. 3. (Color online) The spin-resolved charge-density difference $\Delta\rho(r)=\rho_{\mathrm{Ni/Au-wire}}(r)-[\rho_{\mathrm{Ni}}(r)+\rho_{\mathrm{Au-wire}}(r)]$ for the bridge case and for the substitutional case. The charge flows from black (negative) region to white (positive) region.

bridge case which are even (odd) with respect to the mirror reflection about the xz plane, while Fig. 6 refers to the substitutional case.

In the monatomic Au wire, the s and the $d_{3z^2-r^2}$ states, which have orbital angular momentum $m=0$, lie in a wide energy range and give the main contribution to the Au-Au bonding. The s states are associated with an ideal conductance G_0 of the pristine Au nanowire and contribute with two channels (one per spin) to the transmission even away from the Fermi level. The $|m|=1$ twofold-degenerate bands (linear combination of d_{yz} and d_{zx} states) lie strictly below the Fermi level. In the present geometry and approximation the band edges are at −2.0 and −0.2 eV. Similarly the $|m|=2$ twofold-degenerate bands (linear combination of d_{xy} and $d_{x^2-y^2}$ states) are located around −0.8 eV with a bandwidth of about 0.34 eV.

By comparing the PDOS projected on the Ni atom and on the Au atoms close to Ni we can draw some conclusions on the bonding of Ni to the Au wire. We start by discussing the bridge case. In Fig. 4 one can see that, at energies slightly above 1 eV (with respect to the Fermi level), there are peaks of unoccupied Au s levels both of majority and minority spins. Corresponding peaks are found in the projections on the s states of Ni in both spin channels. The peak above the Fermi level in the Ni s spin-up channel is not present in the isolated atom PDOS and indicates a transfer of charge from the occupied s level of Ni to the wire contributing to the bond. Just above the Fermi level, at about 0.1–0.2 eV, there is the main minority-spin empty state d_{zx} of Ni. It is responsible for giving the bridge Ni impurity essentially a spin 1/2. In GGA+U this spin-down hole state moves well above E_F, giving the bridge impurity a full 1/2 spin. Weak accompanying peaks are present in the PDOS of neighboring Au, suggesting that d_{zx} states of Au also contribute to the bonding.

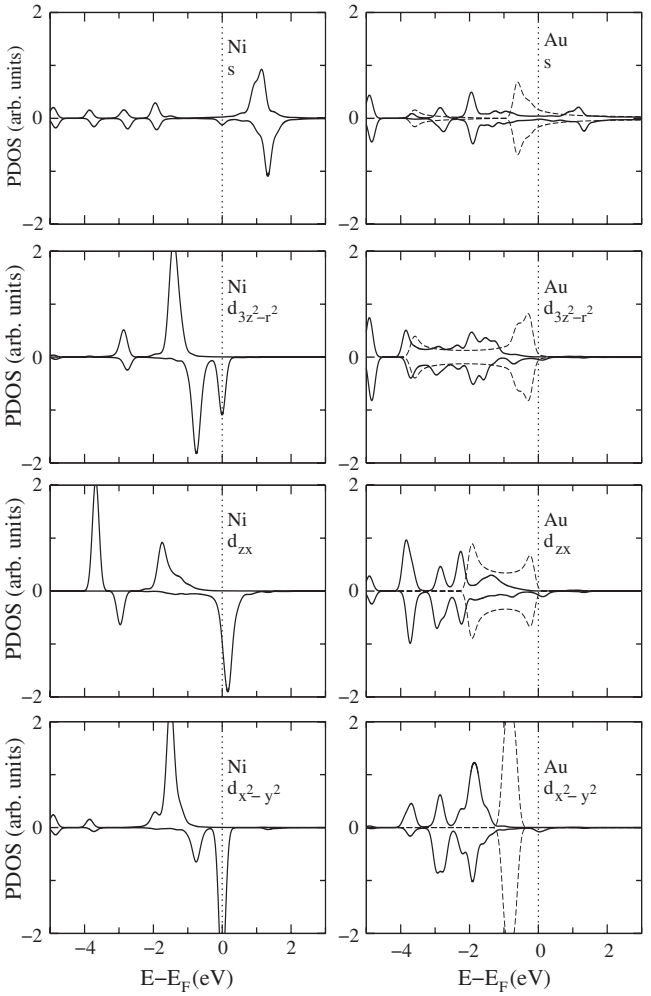

FIG. 4. Projected density of states onto s, $d_{3z^2-r^2}$, d_{zx}, and $d_{x^2-y^2}$ orbitals (even states with respect to mirror reflection about the xz plane) of Ni and of the two Au atoms in contact with Ni, for the bridge case. The PDOS of the monatomic Au wire are also shown (dashed lines).

Au $d_{3z^2-r^2}$ and $d_{x^2-y^2}$ states which are even with respect to the mirror plane containing the Ni atom and the wire, mix with the d_{zx} states of Ni and also have unoccupied states at about the same energies in the minority-spin PDOS. Finally, the PDOS on the d_{yz} and d_{xy} states of Au which are odd with respect to the xz mirror plane, shown in Fig. 5, have no unoccupied states above the Fermi level. However, due to the presence of Ni, these states hybridize and, therefore, the shape of their PDOS changes significantly with respect to the clean wire: new peaks appear at about −3.1, −2.3, and −2.1 eV and corresponding peaks are visible in the Ni PDOS.

The PDOS for the substitutional case are shown in Fig. 6. We can see no unoccupied state in the PDOS on the Au $d_{3z^2-r^2}$ states and no well defined peak in the Au s PDOS. Actually the Ni s PDOS shows a continuum of states above the Fermi level, indicating a good hybridization with the s Au band. This suggests that the Ni s and $d_{3z^2-r^2}$ states make bonds with the $m=0$ states of Au exactly like the orbitals of the Au atom that is substituted and accordingly the effects of

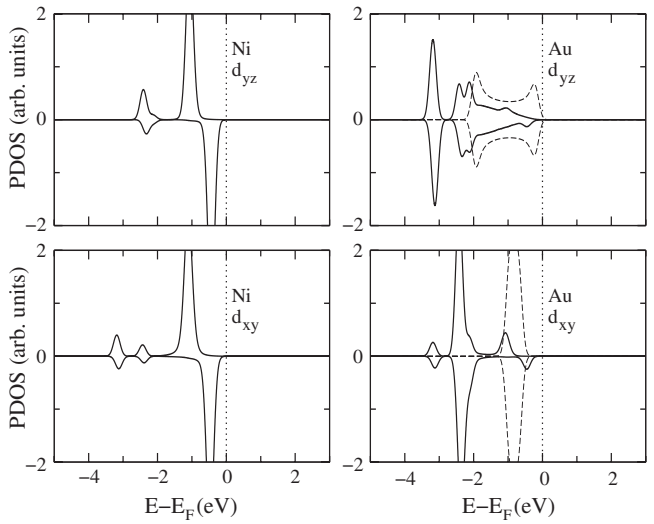

FIG. 5. Projected density of states onto d_{yz} and d_{xy} orbitals (odd states with respect to mirror reflection about the xz plane) of Ni and of the two Au atoms in contact with Ni, for the bridge case. The PDOS of the monatomic Au wire is also shown (dashed lines).

the Ni inclusion into the electronic structure of the Au wire is relatively small. The main source of magnetism now stems from Ni minority spin $|m|=1$ states with symmetry d_{yz} and d_{zx} which lie at the Fermi level but are largely empty. These states are hardly affected by GGA+U; however, in GGA +U the total magnetic moment is slightly larger, $M_{\text{tot}} \sim 2\mu_B$, and Ni can be modeled as a spin 1 impurity. Also Au has a corresponding minor peak in the same symmetry channel indicating an interaction between corresponding states in Ni and Au. The PDOS on the $|m|=2$ Au orbitals show very sharp peaks that are displaced with respect to the peaks of the clean wire and are present also in the corresponding Ni PDOS, albeit less pronounced.

D. Ballistic conductance

In Fig. 7 we show the spin-resolved transmission as a function of the energy of the incident electron for the bridge and substitutional cases. The number of channels available at each energy is also shown for comparison. According to the Landauer-Büttiker theory, in the linear-response regime, the conductance is proportional to the transmission at the Fermi level that we take as the zero of the energy. Here, the Au nanowire has only s states. However, we show the transmission in the range -3.0 eV$<E<3.0$ eV in order to have a clearer picture of the effect of a Ni atom on the ballistic transport in a Au nanowire. In this broader energy range, structures appear in the transmission due to the d states of Au, besides of course the d and s states of Ni.

We start by discussing the bridge case. Above the Fermi level the calculated transmission differs significantly from that of the monatomic Au wire. It is spin dependent, indicating a substantial influence of the Ni impurity. The transmission shows a dip structure at 1.1 eV in the majority-spin channel and at 0.2 and 1.3 eV in the minority-spin channel. The positions of two of these dips correspond to empty state peaks which appear in the PDOS of the Au s states at 1.1 eV

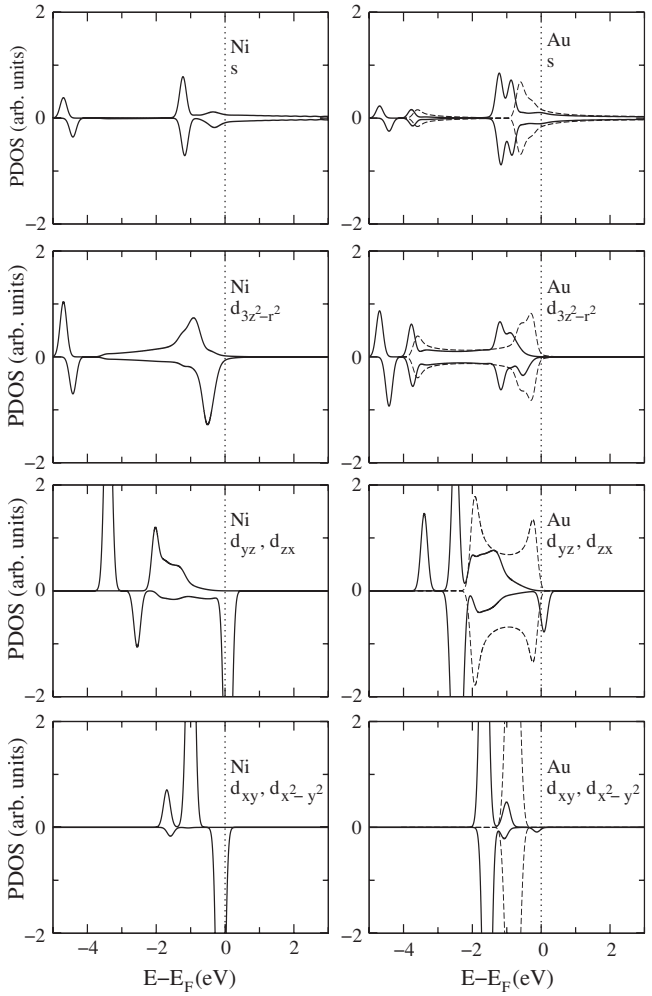

FIG. 6. Projected density of states onto s, $d_{3z^2-r^2}$, (d_{yz}, d_{zx}), and $(d_{xy}, d_{x^2-y^2})$ orbitals of Ni and the two Au atoms in contact with Ni for the substitutional case. The PDOS of the monatomic Au wire are also shown (dashed lines).

for the majority-spin state and at 1.3 eV for the minority-spin state. As noted above, these peaks are present also in the PDOS of the Ni s states which, hybridizing with the Au s states, contribute to block the s-electron conductance of the monatomic Au wire in the energy region that corresponds to the antibonding peaks. The dip at 0.2 eV which appears in the transmission for the minority-spin channel and the difference between the spin-up and spin-down transmissions at the Fermi energy is related to the scattering of the s Au states with the spin-down Ni d_{zx} hole. Some amount of Fano-type interference in these dips may be caused by the possibility of the incoming electron to pass through the scattering region along two routes: one through the impurity (with its resonant levels) and one straight along the Au wire, two waves which in general interfere. Propagating states above the Fermi level in the monatomic Au wire have predominantly s character and they cannot propagate through the scattering region in the energy region where they form a bond with Ni. Since the energy region where the (anti-) bonding peaks appear are different for spin-up and spin-down electrons, the net result is a spin-dependent transmission.

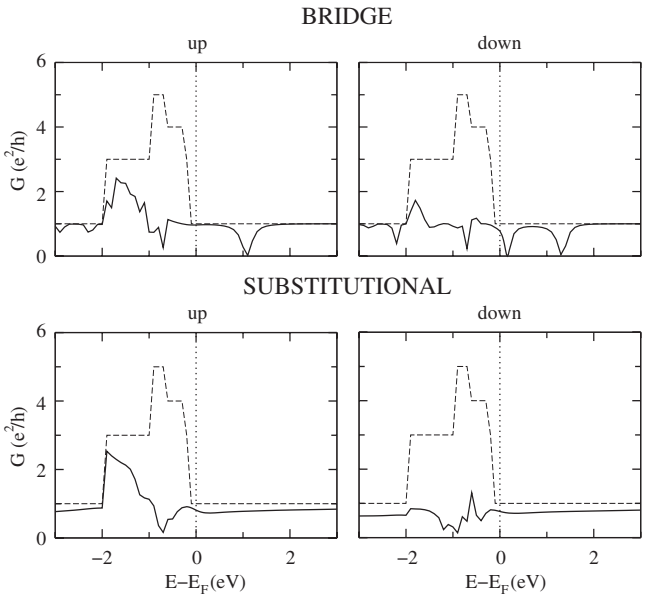

FIG. 7. Majority-spin (left) and minority-spin (right) conductance as a function of energy relative to the Fermi energy for the bridge and substitutional cases. The conductance of a perfect Au wire is also shown (dashed line) for comparison.

The value of the conductance, proportional to the transmission at the Fermi energy, is quite sensitive to the position of the dips close to the Fermi level. In our geometry we find a conductance of 0.78 e^2/h for the spin-minority electrons and 0.96 e^2/h for the spin-majority electrons. However, these values are quite dependent on the very technical and unsafe details of the calculation. In particular inclusion of a self-interaction correction or the addition of a Hubbard-U term in GGA+U can change significantly the position of these dips and therefore influence the conductance (see Sec. IV for a more thorough discussion of this issue).

Below the Fermi level more channels are available for transmission. However, at -2.0 eV$<E<0.0$ eV, the transmission remains low, $1.02\div2.4$ per spin, much lower than the transmission in the clean nanowire ($3.0\div5.0$ per spin). This is due to the fact that the Au nanowire states with predominantly $d_{x^2-y^2}$ and d_{xy} character do not propagate through the scattering region. For -3.0 eV$<E<-2.0$ eV, on the other hand, the transmission is close to the clean-wire value, 1.0. In this energy region the Au propagating states have $d_{3z^2-r^2}-s$ character and contribute to the transmission because of the reduced hybridization with the Ni states.

The transmission for the substitutional case differs qualitatively from the bridge case. A Ni atom in the substitutional position does not block the transmission of the $s-d_{3z^2-r^2}$ channel at the Fermi level. Actually the transmission is nearly independent of spin above the Fermi level and is only slightly reduced with respect to the clean Au wire. The conductance is equal to 0.81 e^2/h and 0.76 e^2/h for spin-majority and spin-minority electrons, respectively. This behavior is in agreement with the fact that the PDOS of Ni s shows a broad tail above the Fermi level indicating a good hybridization with the Au s band.

The spin dependence of the transmission is remarkable at -2.0 eV$<E<-0.2$ eV. In this energy region, Ni $|m|=1$ and $|m|=2$ states make bonds with Au $|m|=1$ and $|m|=2$ states, respectively. Since these Ni states are spin polarized, incident electrons from Au $|m|=1$ and $|m|=2$ undergo spin-dependent scattering.

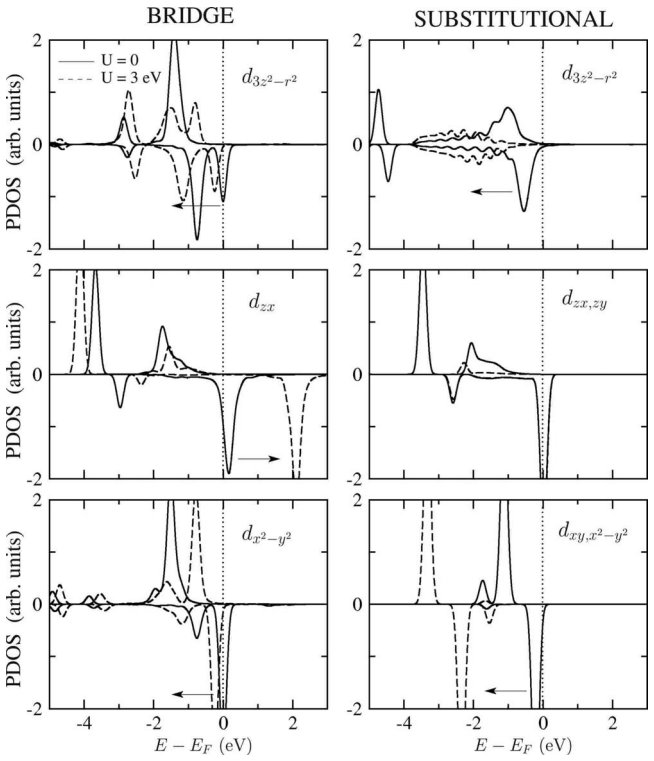

FIG. 8. PDOS onto the Ni d orbitals calculated with $U=3$ eV (dashed lines) compared to the case of $U=0$ (solid lines), corresponding to GGA calculations. The results for bridge and substitutional geometries are shown in the left and right panels, respectively. The arrows indicate the shifts in the positions of some PDOS resonances around the Fermi level due to the inclusion of U. For these calculations, a supercell containing 16 Au atoms was used.

IV. DISCUSSION

As we pointed out in Sec. III, there are many resonances around the Fermi energy in the Ni PDOS shown on the left panels of Figs. 4–6, which correspond to LDA electronic levels, mainly spin-down holes, on the Ni atom. It is well known, however, that due to incomplete cancellation of self-interactions, LDA generally places all states, filled and empty, too close to the Fermi level.[31] One can therefore expect the position of these LDA spin-down empty Ni levels to be unsafe, as they would in general be shifted upward by a better cancellation of self-interactions. In order to get qualitative insight into these effects, we carried out GGA+U calculations within the QUANTUM ESPRESSO package. The details of the GGA+U approach are quite standard, as described, e.g., by Ref. 22. A U correction of 3 eV was applied to the Ni d states only. This parameter value is in line with values adopted in the literature[27] and we did not attempt to determine it with a self-consistent procedure.[22] In Fig. 8 we show how the PDOS of the Ni d orbitals are modified. Since the Hubbard U discourages partial occupancies, it acts

to fill up some partially filled levels and empty out others. In the bridge case, the $d_{3z^2-r^2}$ and $d_{x^2-y^2}$ resonances are pushed down in energy, while the spin-down hole state of d_{zx} symmetry is shifted to higher energies (these shifts are indicated by arrows in Fig. 8). This "cleans up" the energy region around the Fermi level and yields an integer magnetic spin moment of $1.0\mu_B$ (instead of $1.30\mu_B$, the value obtained by GGA calculations), corresponding to a spin 1/2 system with one hole. A similar action of GGA+U is found in the substitutional Ni geometry, with the difference that the position of the two $d_{zx,zy}$ degenerate spin-down hole levels remains practically unchanged. While they remain pinned just above the Fermi energy, the magnetic moment is now $2.02\mu_B$, compared with the GGA value of $1.91\mu_B$, describing a spin 1 system. As far as the ballistic conductance is concerned, we expect that GGA+U will not change qualitatively the picture described in Sec. III. In the substitutional case, we expect it to be still slightly lower than e^2/h for each spin channel. In the bridge geometry, the spin-down conductance was lower than e^2/h ($0.78\ e^2/h$) in our GGA calculations due to the presence of the Ni d_{zx} state, which affected the density of states (DOS) of nearest-neighbor Au atoms. Since this level is shifted significantly by U from the Fermi level to higher energies, we can argue that the conductance of the spin-down channel should recover a value close to e^2/h.

V. CONCLUSIONS

We investigated the structural, electronic, and magnetic properties of a Ni impurity on a monoatomic Au wire and discussed the ballistic conductance of the system. First, we found that the Ni atom predominantly adsorb at the bridge site in a monatomic Au wire at the chosen Au-Au distance, $d_a=2.80$ Å. Second, we showed that in the bridge case, above the Fermi level, the transmission of the $m=0$ channel has dips at the energies of the unoccupied antibonding states of the Ni-Au s orbitals. Furthermore the hybridization of the even d_{zx} states of Ni with the even states of Au also produces a blocking of the $m=0$ channel near E_F. Due to this blocking effect, the transport properties of this system at the Fermi level become very sensitive to the exact position of the antibonding states and therefore are quite difficult to predict exactly. In our geometry and in the GGA approximation the spin-up conductance is very close to the perfect-wire value, e^2/h, whereas the spin-down conductance is reduced. However, the addition of a Hubbard-U term shifts the d_{zx} levels up in energy and, as a consequence, the spin-down conductance is expected to be close to e^2/h as well. On the other hand, the Ni on the substitutional site hardly changes the G_0 transmission above the Fermi level.

We therefore conclude that the transmission is sensitive to the position of the Ni atom on the monatomic Au wire and can become spin dependent. The position of the dips in transmission are strongly dependent on the impurity atom because they depend on the hybridization between the states of the impurity and the s states of the wire. How much an external stress applied to the wire or the presence of the tips change this picture will be the subject of future investigations.

Our results for an idealized nanowire system are difficult to compare directly with existing experiments. Nonetheless, they indicate a very different spin state for a Ni impurity adsorbed onto, or embedded into, a monatomic Au nanocontact. They additionally suggest the possibility that when the G_0 conductance of Au nanocontacts remains unchanged in presence of transition-metal impurities,[11] that should not necessarily imply that the impurities play no role, or are not magnetic.

When comparing with future experiments, it will be important to note that strong thermal and quantum fluctuations, and in particular Kondo effects, will influence importantly the zero-voltage electron conductance. A proper inclusion of these effects remains a task for the future, and in fact we expect that the present calculation will serve as the basis for that development. The present type calculation still retains a strong direct value for all situations where fluctuations can be removed or canceled. Besides the hypothetical and probably unrealistic case of an ultrastrong external magnetic field, frozen moments should represent an acceptable approximation to the conductance at voltages above typical Kondo energies. An evaluation of the Kondo energy scale is presently beyond our goals, but we expect it to be typically in the meV range. Therefore, comparison of our Landauer ballistic conductance results with experiments should be sought at voltages just above the possible zero-bias anomalies.[32] Of course, inelastic channels will also open up and influence the conductance at finite voltage[33–35] and care should be taken not to mistake the two different effects.

Finally, we would like to mention that the presence of the impurity might induce anisotropic magnetoresistance effects[36–38] when a magnetic field is applied; to address these effects the spin-orbit coupling, which was not included in our calculations, should be taken into account.

ACKNOWLEDGMENTS

We are grateful to H. Akinaga for useful discussions and comments on our work. This work was supported in part by the New Energy and Industrial Technology Development Organization (NEDO) under the Nanotechnology Materials Program in Japan. Y.M. gratefully acknowledges support from a Grant-in-Aid for Scientific Research of the Japanese ministry of Education, Culture, Sports, Science and Technology (Grant Nos. 17064001, 18760227, and 19048002), and hospitality in SISSA where part of this work was performed. Work at SISSA was supported by Italian Ministry of University and Research, through Grant No. PRIN-2006022847, and by INFM through "Iniziativa Trasversale Calcolo Parallelo."

*mazzarel@sissa.it

[1] N. Agraït, A. L. Yeyati, and J. M. van Ruitenbeek, Phys. Rep. **377**, 81 (2003).
[2] L. Olesen, E. Laegsgaard, I. Stensgaard, F. Besenbacher, J. Schiøtz, P. Stoltze, K. W. Jacobsen, and J. K. Nørskov, Phys. Rev. Lett. **72**, 2251 (1994).
[3] M. Brandbyge, J. Schiøtz, M. R. Sørensen, P. Stoltze, K. W. Jacobsen, J. K. Nørskov, L. Olesen, E. Laegsgaard, I. Stensgaard, and F. Besenbacher, Phys. Rev. B **52**, 8499 (1995).
[4] H. Ohnishi, Y. Kondo, and K. Takayanagi, Nature (London) **395**, 780 (1998).
[5] V. Rodrigues, J. Bettini, A. R. Rocha, L. G. C. Rego, and D. Ugarte, Phys. Rev. B **65**, 153402 (2002).
[6] H. Oshima and K. Miyano, Appl. Phys. Lett. **73**, 2203 (1998).
[7] T. Ono, Y. Ooka, H. Miyajima, and Y. Otani, Appl. Phys. Lett. **75**, 1622 (1999).
[8] V. Rodrigues, J. Bettini, P. C. Silva, and D. Ugarte, Phys. Rev. Lett. **91**, 096801 (2003).
[9] C. Untiedt, D. M. T. Dekker, D. Djukic, and J. M. van Ruitenbeek, Phys. Rev. B **69**, 081401(R) (2004).
[10] A. Smogunov, A. Dal Corso, and E. Tosatti, Phys. Rev. B **70**, 045417 (2004).
[11] A. Enomoto, S. Kurokawa, and A. Sakai, Phys. Rev. B **65**, 125410 (2002).
[12] D. J. Bakker, Y. Noat, A. I. Yanson, and J. M. van Ruitenbeek, Phys. Rev. B **65**, 235416 (2002).
[13] N. Papanikolaou, J. Opitz, P. Zahn, and I. Mertig, Phys. Rev. B **66**, 165441 (2002).
[14] K. Palotas, B. Lazarovits, L. Szunyogh, and P. Weinberger, Phys. Rev. B **70**, 134421 (2004).
[15] R. B. Pontes, E. Z. da Silva, A. Fazzio, and A. J. R. da Silva, J. Am. Chem. Soc. **130**, 9897 (2008).
[16] S. R. Bahn and K. W. Jacobsen, Phys. Rev. Lett. **87**, 266101 (2001).
[17] E. Z. da Silva, F. D. Novaes, A. J. R. da Silva, and A. Fazzio, Phys. Rev. B **69**, 115411 (2004).
[18] S. Datta, in *Electronic Transport in Mesoscopic System*, Cambridge Studies in Semiconductor Physics and Microelectronic Engineering (Cambridge University Press, Cambridge, 1995).
[19] H. J. Choi and J. Ihm, Phys. Rev. B **59**, 2267 (1999).
[20] A. Smogunov, A. Dal Corso, and E. Tosatti, Phys. Rev. B **73**, 075418 (2006).
[21] D. Vanderbilt, Phys. Rev. B **41**, 7892 (1990).
[22] M. Cococcioni and S. de Gironcoli, Phys. Rev. B **71**, 035105 (2005).
[23] J. P. Perdew, K. Burke, and M. Ernzerhof, Phys. Rev. Lett. **77**, 3865 (1996).
[24] S. Baroni, A. Dal Corso, S. de Gironcoli, and P. Giannozzi (http://www.quantum-espresso.org).
[25] M. Methfessel and A. T. Paxton, Phys. Rev. B **40**, 3616 (1989).
[26] A. Delin and E. Tosatti, Phys. Rev. B **68**, 144434 (2003).
[27] M. Wierzbowska, A. Delin, and E. Tosatti, Phys. Rev. B **72**, 035439 (2005).
[28] G. Rubio-Bollinger, S. R. Bahn, N. Agrait, K. W. Jacobsen, and S. Vieira, Phys. Rev. Lett. **87**, 026101 (2001).
[29] E. Tosatti, Solid State Commun. **135**, 610 (2005).
[30] A. Smogunov, A. Dal Corso, and E. Tosatti, Surf. Sci. **507–510**, 609 (2002).
[31] J. P. Perdew and A. Zunger, Phys. Rev. B **23**, 5048 (1981).
[32] P. Wahl, L. Diekhöner, M. A. Schneider, L. Vitali, G. Wittich, and K. Kern, Phys. Rev. Lett. **93**, 176603 (2004).
[33] T. Frederiksen, M. Brandbyge, N. Lorente, and A. P. Jauho, Phys. Rev. Lett. **93**, 256601 (2004).
[34] L. Stella, G. E. Santoro, M. Fabrizio, and E. Tosatti, Surf. Sci. **566–568**, 430 (2004).
[35] L. de la Vega, A. Martín-Rodero, N. Agraït, and A. L. Yeyati, Phys. Rev. B **73**, 075428 (2006).
[36] M. Viret, S. Berger, M. Gabureac, F. Ott, D. Olligs, I. Petej, J. F. Gregg, C. Fermon, G. Francinet, and G. Le Goff, Phys. Rev. B **66**, 220401(R) (2002).
[37] J. Velev, R. F. Sabirianov, S. S. Jaswal, and E. Y. Tsymbal, Phys. Rev. Lett. **94**, 127203 (2005).
[38] M. Viret, M. Gabureac, F. Ott, C. Fermon, C. Barreteau, G. Autès, and R. Guirado-Lopez, Eur. Phys. J. B **51**, 1 (2006).